

ANALYSIS OF STRESS AND STRAIN CONCENTRATIONS IN NOTCHED MEMBERS MADE OF ALLOYS D16 AND 1460

Lucjan Śnieżek¹, Jerzy Malachowski²

¹Institute of Machine Design

²Institute of Materials Science and Applied Mechanics

Faculty of Mechanics

Military University of Technology

Key words: notch effect, stress concentration, aluminum alloys.

A b s t r a c t

The aim of the study was to present findings on the effect of the presence of a notch upon stress and strain concentrations in model members for aeronautical structures, made of selected aluminum alloys, i.e. D16 and 1460. Flat specimens with centrally positioned holes and side cuts, loaded with some bending moment of stress ratio $R = 1$, were tested. Specialized FEM software (MSC.Patran and MSC.Nastran) was applied to examine stress and strain distributions. The findings are presented in the form of σ_{\max} and ε_{\max} values as well as functions of the following factors: α_{σ} , α_{ε} , and α_k , computed on the grounds of these values for both different distances from the bottom of the notch and assumed levels of load put on the specimens. Theoretical analysis was supplemented with experimental investigations into the microstructure of fatigue-fracture surfaces in the area of crack initiation and in that of fatigue of a propagating crack.

ANALIZA SPIĘTRZENIA NAPRĘŻENIA I ODKSZTAŁCENIA W ELEMENTACH Z KARBEM WYKONANYCH ZE STOPÓW D16 I 1460

Lucjan Śnieżek¹, Jerzy Malachowski²

¹Istytut Budowy Maszyn

²Instytut Mechaniki Technicznej i Materiałoznawstwa

Wydział Mechaniczny

Wojskowa Akademia Techniczna

Słowa kluczowe: działanie karbu, spiętrzenie naprężenia, stopy aluminium.

S t r e s z c z e n i e

Przedstawiono wyniki badań wpływu działania karbu na spiętrzenie naprężenia i odkształcenia w elementach modelowych wykonanych z wybranych lotniczych stopów aluminium D16 i 1460. Badaniom poddano próbki płaskie z otworem centralnym z nacięciami bocznymi, obciążone momentem zginającym o współczynniku asymetrii cyklu $R = -1$. Do badań rozkładu naprężenia i odkształcenia zastosowano specjalizowane oprogramowanie MES (MSC. Patran i MSC. Nastran). Wyniki obliczeń przedstawiono w postaci zestawienia wartości σ_{\max} , ε_{\max} oraz wyliczonych na ich podstawie przebiegów współczynników α_{σ} , α_{ε} i α_k , w różnej odległości od dna karbu i dla przyjętych poziomów obciążenia próbek. Analizę teoretyczną uzupełniono doświadczalnymi badaniami mikrobudowy powierzchni przełomów zmęczeniowych w strefie inicjacji oraz w strefie zmęczeniowej propagującego pęknięcia.

Introduction

Any analysis of the phenomena which occur where geometric and structural discontinuities (generally called ‘notches’) are found, proves more difficult especially in the case of loads producing low-cycle fatigue. Stress concentration at the bottom of a notch often provokes some plastic strain of the material in this area, which – in the case of cyclic loads – results in both the origination of internal stresses and a change in the mean stress (KOCANĀDA, KOCANĀDA 1989). For many years the effects of some local yielding-inducing stress concentrations upon the fatigue behavior of materials and structural components have been studied at numerous research centers worldwide (PETERSON 1974, HERTZBERG 1983, PILKEY 1997, *Notch Effects...* 2000). It is extremely difficult to take this phenomenon into account in strength computations, especially while using analytical solutions expected to comprise its 3D nature, a complicated shape of the notch, and the effect of boundary conditions. The determination of the actual stress and strain levels in the region of fatigue crack initiation would considerably facilitate the interpretation of the phenomena that accompany the process, as well as enable a description of fatigue cracking of the tested members with stress concentrators in the form of suitably cut crack initiators (ANDREWS, GIBSON 2001, STRANDBERG 2002, TROYANI et al 2004, TLILAN et al 2005). The application of a numerical method offers a chance to find some approximate solution to the above-described problem, however, with some limitations. Among various available methods, the finite element method (FEM) is the most common technique suitable for solving the problem under consideration (ZIENKIEWICZ 1972, DACKO et al 1994). Professional software proves of great assistance while solving problems with this method. However, good knowledge of the FEM theory and some experience in computer modeling are needed. The evaluation of fatigue strength and resistance to cracking is probably the most fundamental criterion, playing a decisive role while selecting

alloys to be used in certain constructions (e.g. aircraft). Along with the progress in designing/developing high-risk structures, modified design methods are introduced, e.g. safe-life and fail-safe concepts, as well as new material production technologies. They are based on new material characteristics which include, among others, an extended approach to mechanisms underlying both crack propagation and the effect of notch dimensions on the crack propagation rate, i.e. the factors expected to ensure the required fatigue life of the structure of a given construction. Apart from investigating the mechanical properties of these materials, much more intense efforts have been made recently to take account of a notch in the structural member under examination (SPENCER et al 2002, TOKAJI 2005).

Therefore, the objective of the study was to determine the effect of a geometric notch in the form of a centrally positioned slot upon the actual values of stresses and strains in flat specimens made of selected aluminum alloys for aircraft structures. The specimens were subjected to variable bending. The findings presented in the paper represent a part of extensive theoretical studies and experimental work on the fatigue cracking of aluminum alloys for aeronautical structures, with account taken of macroscopic plastic strains.

Specimens and methodology of work

Materials and specimens

Specimens made of aluminum alloys D16 and 1460 whose chemical composition is presented in Table 1 were analyzed. These alloys are applied in very reliable members of aeronautical and space structures. The requirements specified for alloys of this type usually have to be followed with investigation into the effects of different material, structural and operational factors on the fatigue properties thereof.

T a b l e 1

Chemical compositions of the alloys under examination

Alloy	Li	Cu	Zr	Mg	Si	Mn	Ti	Al
	weight %							
D16	–	2.99	–	2.18	1.40	0.38	0.18	rest
1460	2.30	2.90	0.13	0.05	–	–	0.05	rest

After rolling, the alloys were subjected to heat treatment that involved solution hyper-quenching and ageing.

Testing work to investigate static mechanical properties was conducted using the Instron 8802 machine and flat specimens cut out in the direction of sheet rolling. The results of these tests are presented in Table 2.

Table 2

Strength properties of the alloys under examination

Alloy	$R_{0.2}$ (MPa)	R_m (MPa)	E (MPa)	Z (%)	A (%)
D16	334	461	67576	15	22
1460	383	458	78740	8.2	4.2

Flat specimens of dimensions shown in Fig. 1 were used in the essential testing work. They were cut out in the direction of sheet rolling. Slots were cut out in the form of centrally located holes, 3 mm in diameter, with side cuts of a total length of 6 mm (see Detail *C* in Fig. 1). These were crack initiators. The outlines of cut tips and the radius of the notch bottom are illustrated with Detail *D*. The size of the radius of the notch bottom, $R = 0.08$ mm, was reached using a suitably profiled hook tool.

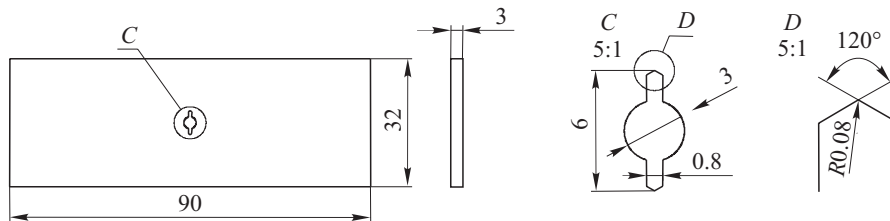


Fig. 1. Dimensions of specimens

Methodology of work

Highly specialized FEM software (MSC.Patran and MSC.Nastran) was used to determine stress and strain distributions. In the first step, a geometric model of a half-specimen was made, with a notch being a crack initiator well represented. In the next step, the mesh model found was created by means of Hex elements. A total number of elements used was 35 456 (Fig. 2).

The FEM mesh was compacted around the notches where strong stress concentration is generated. The boundary conditions assumed in the calculations resulted from specimen symmetry, conditions of fitting them to the test station, and the performed loading which produced the bending effect – at one end the test bar was subjected to bending by force, whereas at the opposite end it was fixed.

The next step in the algorithm of numerical calculations was to introduce the material properties of the structure under analysis. Complete characteristics in the form of a curve $\sigma = f(\varepsilon)$ were used in the calculations. The Huber-Mises condition was assumed as a criterion of the plastic yielding of the material. While performing computations with MSC/Nastran, the basic system of

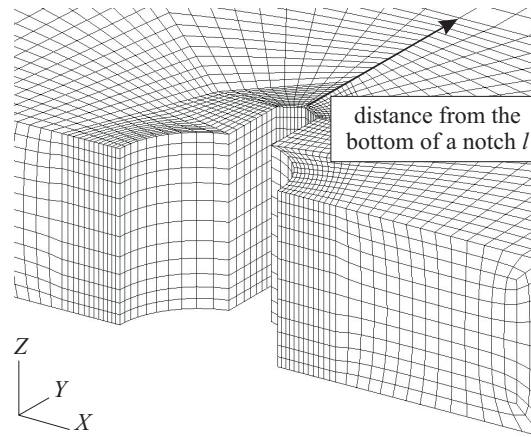


Fig. 2. A discrete FEM model assumed for analysis

differential equations was applied to describe the equilibrium of a loaded elastic-plastic body (SPENCER et al 2002, TOKAJI 2005). The tangential matrix present in the matrix equation of equilibrium is the so-called elastic-plastic matrix, which results from the incremental form of the constitutive law.

The finite element method (FEM) offers procedures that facilitate solving non-linear problems. They can be grouped into three classes: incremental (step-by-step), iterative (*Newton-Raphson's*, *Broyles-Fletcher-Goldfarb-Shanno* – BFGS), and mixed (incremental/ iterative, step-by-step/iterative) procedures. The *Newton-Raphson's* method, quickly convergent with respect to the number of iterations, was used. However, in each iteration a new tangential matrix of stiffness is created, which extends the time needed for computations.

The values of the amplitude of nominal bending stresses σ_{gna} assumed for the purpose of analysis result from the range of specimen loading in the experimental work. The tests were carried out under flat-bending conditions, at the amplitude of nominal bending stresses $\sigma_{\text{gna}} = 80, 90, \text{ and } 100 \text{ MPa}$ (alloy D16) and $\sigma_{\text{gna}} = 70, 100, \text{ and } 200 \text{ MPa}$ (alloy 1460), and the stress ratio $R = -1$.

The mechanism of fatigue crack propagation was traced by means of examining the microstructures of fracture surfaces with a TEM JEOL JEM 1230 microscope, using carbon-sprayed and platinum-shaded acetyl-cellulose replicas.

Results of computations

The conducted numerical analysis facilitated the solving of the problem of

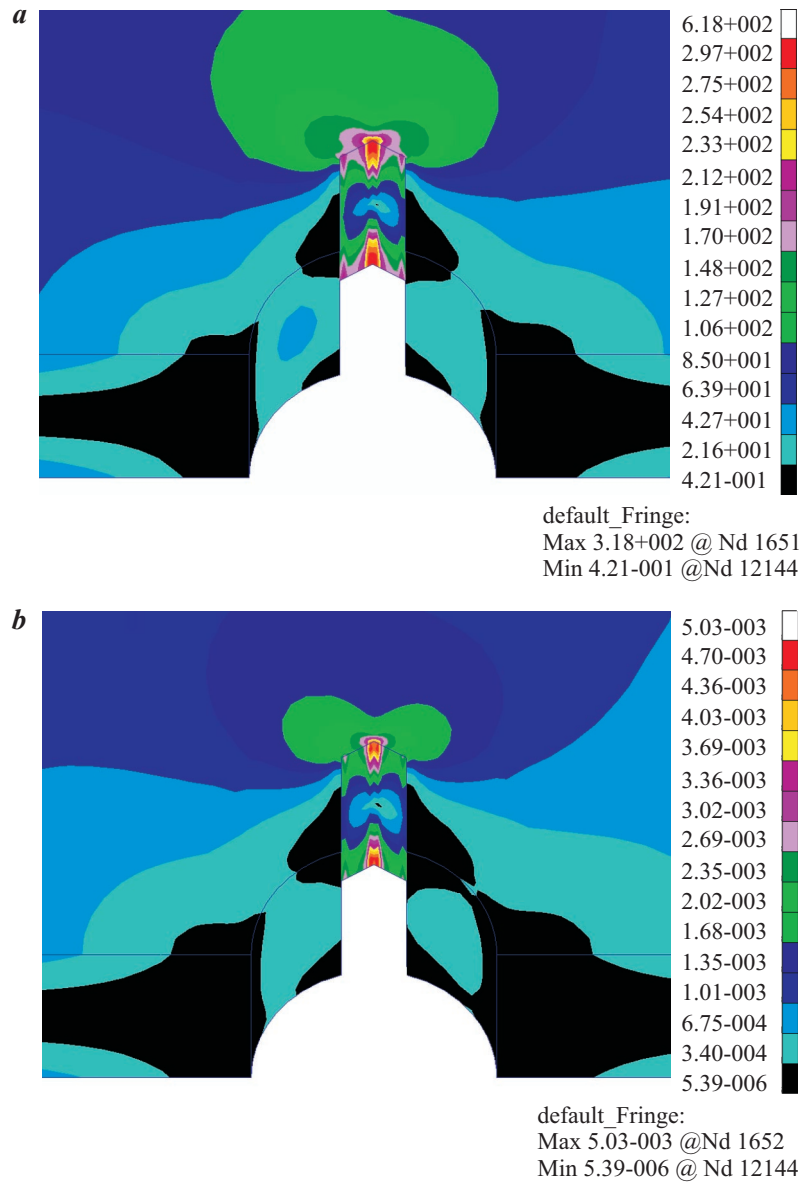


Fig. 3. Distribution of: *a* – reduced stresses, *b* – plastic strains in the notch-affected area in a specimen of alloy D16, examined at $\sigma_{\text{gna}} = 100$ MPa

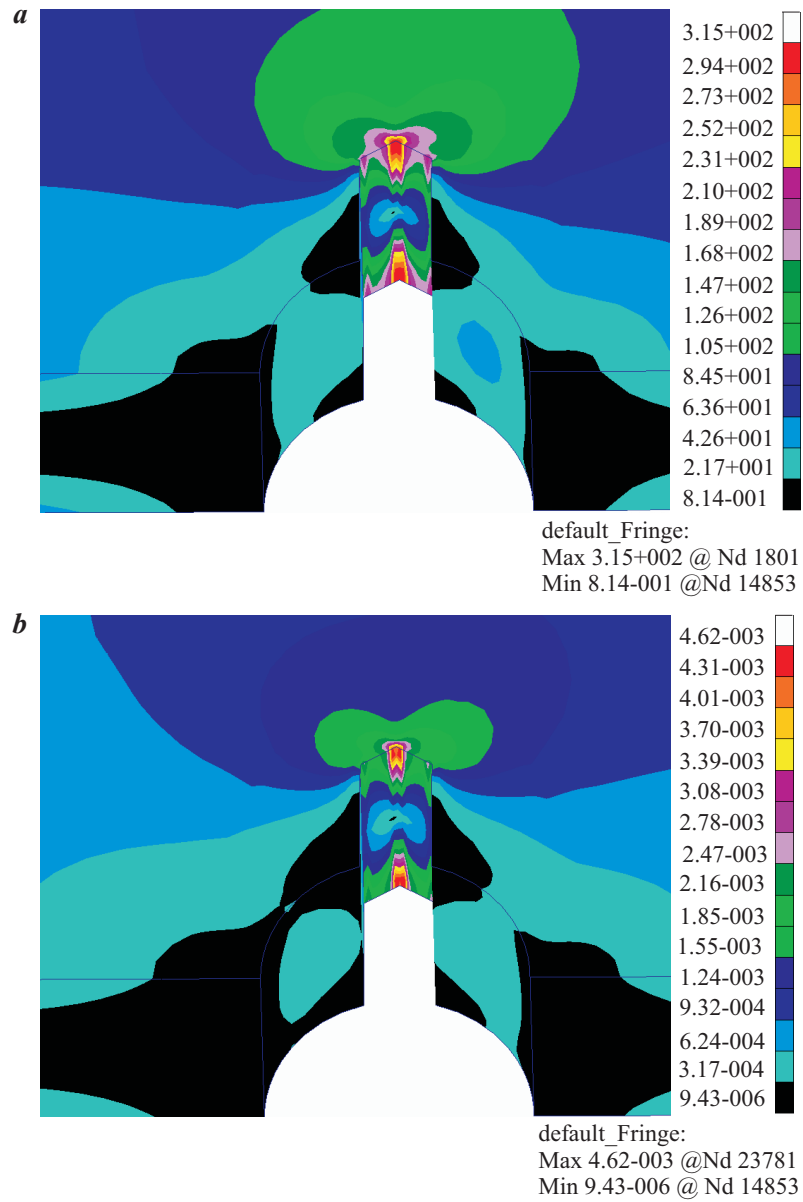


Fig. 4. Distribution of: *a* – reduced stresses, *b* – plastic strains in the notch-affected area in a specimen of alloy 1460, examined at $\sigma_{\text{gna}} = 100$ MPa

stress and strain concentrations around notches. Figs. 3 and 4 show some computational results in the form of maps of reduced stresses and plastic strains in the areas of notches made in the specimens of alloys D16 and 1460, at the amplitude of nominal bending stresses $\sigma_{gna} = 100$ MPa. Using these maps, curves of total strains ε_c were plotted for different values of σ_{gna} , depending on the

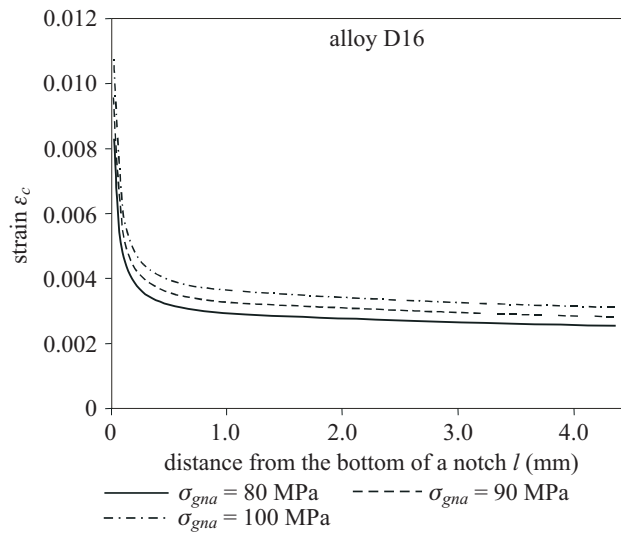


Fig. 5. Distribution of total strain $\varepsilon_c = f(l)$ in components made of alloy D16

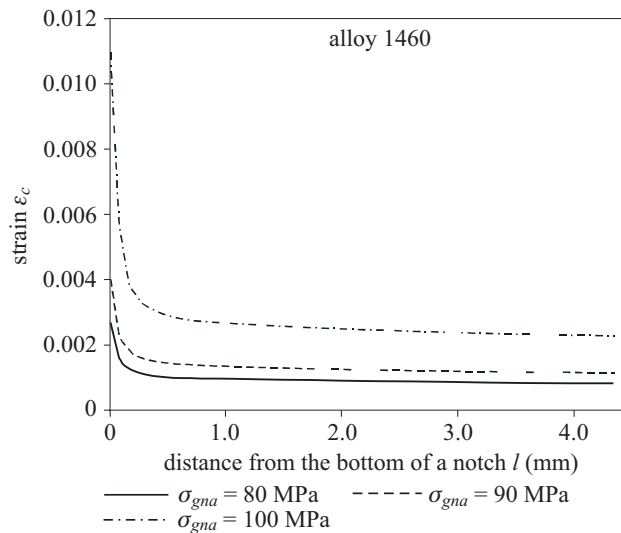


Fig. 6. Distribution of total strain $\varepsilon_c = f(l)$ in components made of alloy 1460

distance l from the bottom of the notch cut out in the direction shown in Fig. 2 (Figs 5 and 6).

The results of computations of the amplitude of the actual bending stress σ_{ga} and the corresponding total strain ϵ_c depending on the distance l from the notch,

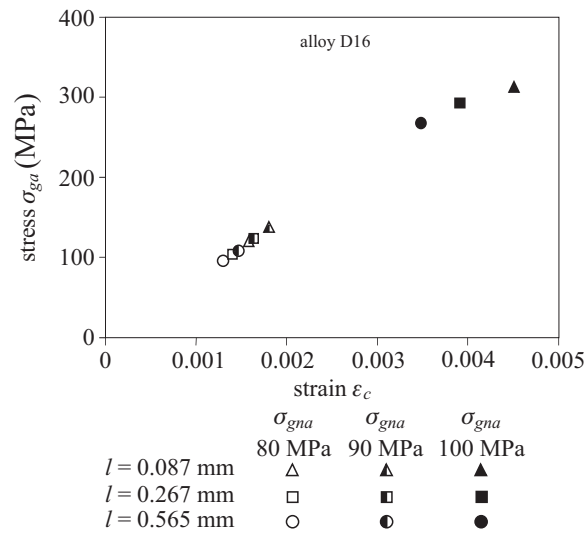


Fig. 7. Results of calculations performed for stress σ_{ga} and strain ϵ_c in components made of alloy D16

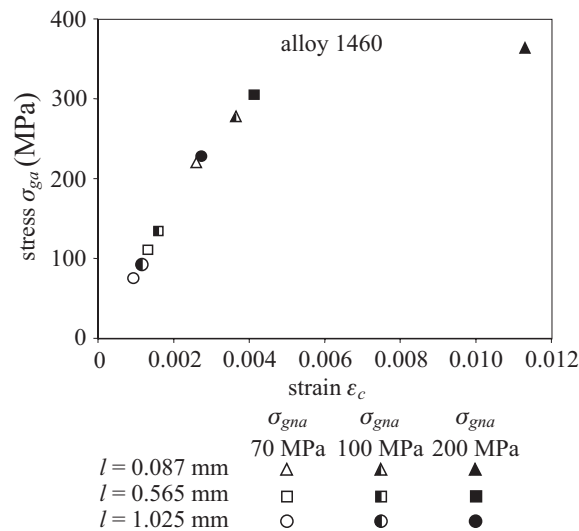


Fig. 8. Results of calculations performed for stress σ_{ga} and strain ϵ_c in components made of alloy 1460

for different values of the amplitude of the nominal bending stress σ_{gna} , are presented in Figs. 7 and 8.

The observed stress and strain concentrations, α_σ and α_ε respectively, decrease rapidly as the distance from the bottom of the notch increases. The intensity of these concentrations can be determined using the shape factor α_k , which – according to the H. Neuber’s concept (KOCAŃDA, KOCAŃDA 1989) – is a geometric mean of factors α_σ and α_ε :

$$\alpha_k^2 = \alpha_\sigma \cdot \alpha_\varepsilon \quad (1)$$

with $\alpha_\sigma = \frac{\sigma_{\text{max}}}{\sigma_n}$, and $\alpha_\varepsilon = \frac{\varepsilon_{\text{max}}}{\varepsilon_n}$.

Table 3

Values of σ_{max} and ε_{max} , and factors α_σ , α_ε , α_k for notches made in specimens made of alloys D16 and 1460

Alloy	σ_{gna} (MPa)	σ_n	σ_{max} (MPa)	σ_{max}	α_σ	α_ε	α_k
D16	80	0.0026	410	0.0083	5.125	3.192	4.045
	90	0.0029	440	0.0095	4.889	3.276	4.002
	100	0.0032	460	0.0108	4.600	3.375	3.940
1460	70	0.0009	240	0.0028	3.429	3.111	3.266
	100	0.0012	305	0.0040	3.000	3.333	3.188
	200	0.0024	370	0.0110	1.850	4.583	2.912

In the expressions above, σ_{max} and ε_{max} are maximum values of local stresses and strains, and σ_n and ε_n are nominal values thereof. The values σ_{max} and ε_{max} found with the finite element method, and factors α_σ , α_ε , α_k calculated on the grounds of these values for notches cut out in specimens made of alloys D16 and 1460, are presented in Table 3.

As loading increases, the values of α_σ , α_ε , and consequently, α_k , change in the way shown in Figs. 9 and 10. The nominal stresses accepted in the course of analysis of alloy D16, i.e. $\sigma_{\text{gna}} = 80 - 100$ MPa, provoked considerable stress concentration in the area of the notch tip. This stress concentration was greater (for the entire range of the applied loads) than the strain concentration. This affected the value of the shape factor calculated for specimens made of this alloy, i.e. $\alpha_k = 3.940 - 4.045$. The results of calculations for alloy 1460, made at $\sigma_{\text{gna}} > 100$ MPa (Fig. 10), confirmed the argument contained in [1] that the plastic flow of the material limits the value of the stress concentration factor α_σ , which cannot be said about the strain concentration factor α_ε . The plastic flow

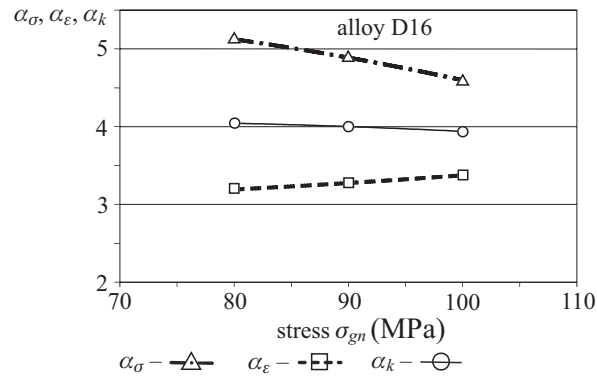


Fig. 9. Stress and strain concentrations in the area of the bottom of a notch cut in a member made of alloy D16

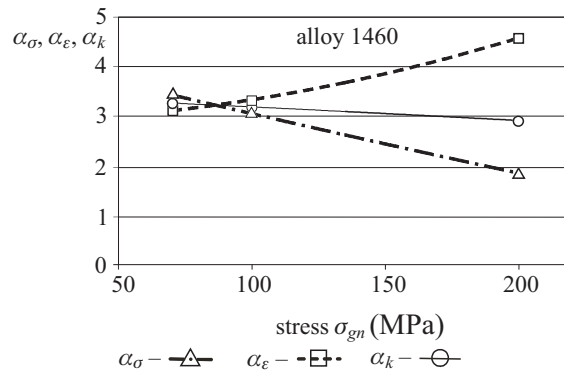


Fig. 10. Stress and strain concentrations in the area of the bottom of a notch cut in a member made of alloy 1460

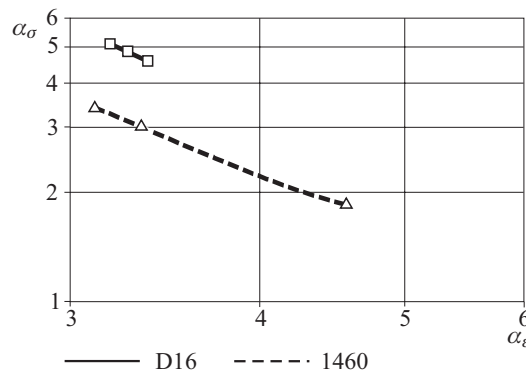


Fig. 11. Comparison of the values of as and ae calculated for members made of alloys D16 and 1460

of the material considerably increases the maximum local strain, and consequently, α_ε . Therefore, under conditions featured with macroscopic plastic strains, the level of α_ε can prove of greater significance than that of α_s . The calculated values of the shape factors for specimens made of alloy 1460 were lower than those calculated for alloy D16 alloy ($\alpha_k = 2.912 - 3.266$).

Microstructures of fatigue fracture surfaces

In the course of fatigue tests, cracks were always initiated at the bottom of the cut out notch, regardless the pre-stress level; the direction of propagation coincided with the plane of maximum normal stresses.

The micrographs obtained with a transmission electron microscope (TEM) delivered information on the mechanism of cracking in the tested specimens. Some sections of fractures shown in Fig. 12 come from specimens made of alloys D16 and 1460, tested at $\sigma_{\text{gna}} = 100$ MPa.

Within the notch, in the area of stress and strain concentrations, there are micro-areas that differ from typical fatigue fractures and well illustrate the mechanism of quick fatigue failing of the material (Figs. 12a and 12c). What is meant is the rapidity of changes taking place, and of the process of cracking. It is manifested with a complex microstructure of a fracture in a specimen made of alloy D16, with local shearing of surface bands and numerous fracture-induced fissures. Fig. 12a shows jogs that prove a crack to snap through between planes of growth of many microcracks which propagate in adjacent layers of the strongly deformed structure of the alloy under examination. The jogs appeared due to the shearing or breaking of bridges which separate planes of cracking from each other.

Some section of the fracture surface taken from the cracking-initiation area in 1460 alloy specimen shows features of brittle cracking, such as local cleavage and quasi-cleavage fractures interspersed with features of ductile cracking. Obviously, in the case of aluminum alloys under examination it is difficult to generally talk about cleavage cracking; however, these are features of a locally high rate of cracking at the initial stage of cracking propagation.

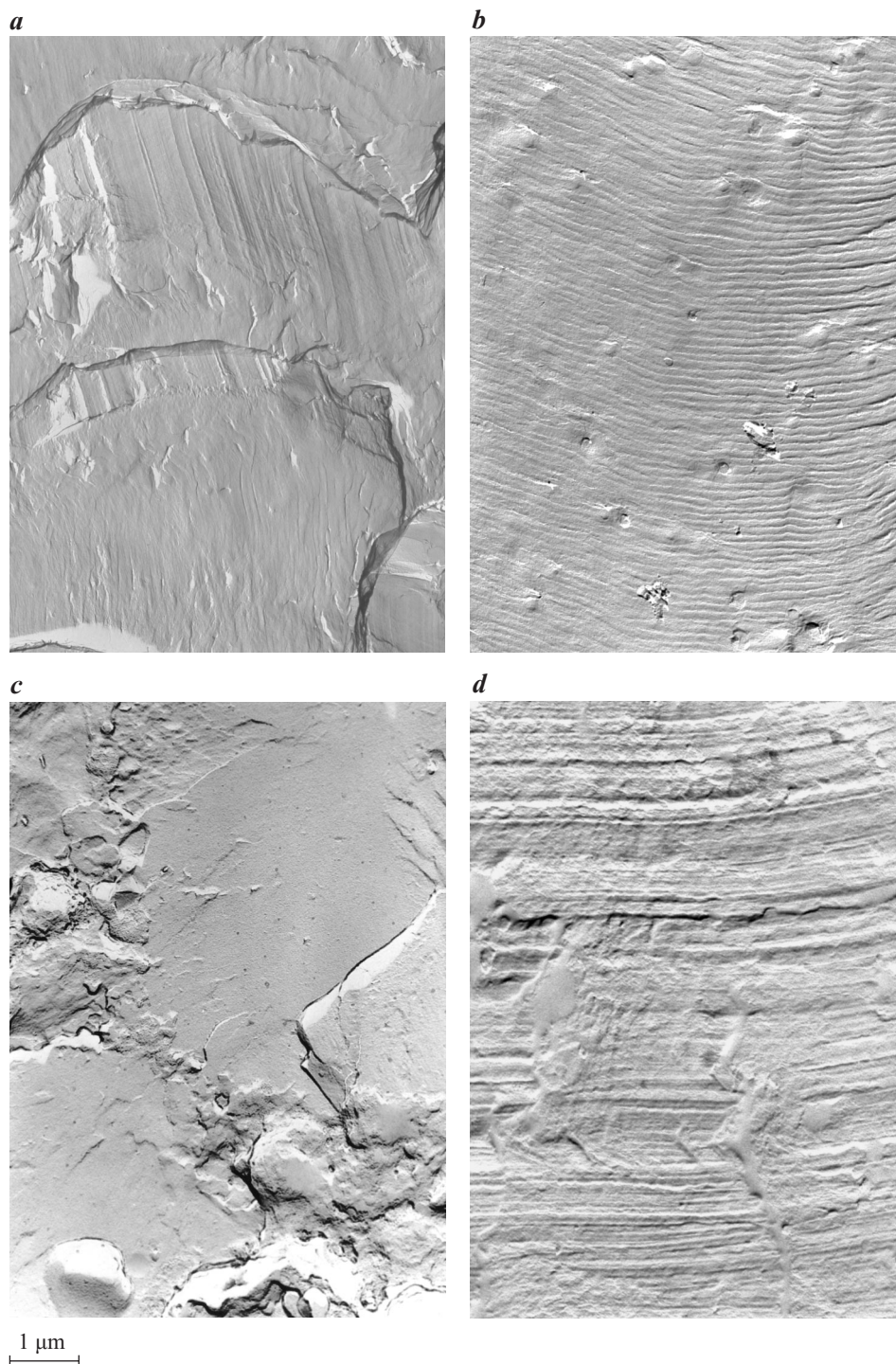


Fig. 12. Initiation (*a*, *c*) and fatigue (*b*, *d*) areas of crack growth and propagation in specimens made of alloys D16 (*a*, *b*) and 1460 (*c*, *d*), at $\sigma_{\text{gna}} = 100$ MPa

The fracture microstructure changes in the fatigue area. At the distance of approximately 0.4 mm from the bottom of the notch, a band of plastic and irregular fatigue striations appears (Figs 12b and 12c). In 1460 alloy specimen these striations were rather poorly visible (Fig. 12d). Noticeable differences in inter-striation distances at the same depth prove local changes in cracking rates.

Summary

The findings presented in the paper are the source of information on the effect of a notch, in the form of a centrally positioned hole with side cuts, upon levels of stress concentrations in flat bars made of aeronautical aluminum alloys D16 and 1460, subjected to flat bending. The values of shape factors were $\alpha_k = 3.940 - 4.045$ (for the range of $\sigma_{\text{gna}} = 80 - 100$ MPa) for alloy D16, and $\alpha_k = 2.912 - 3.266$ (for the range of $\sigma_{\text{gna}} = 70 - 200$ MPa) for alloy 1460. For the range of $\sigma_{\text{gna}} = 80 - 100$ MPa, the shape factor for specimens made of alloy D16 proves 23–25% greater than that calculated for alloy 1460. The observed behavior of the alloys under examination resulted first and foremost from differences in both chemical composition and structure thereof, which in turn were affected by different processes of manufacture. In consequence, dissimilar strength properties were gained. Alloy 1460, included in the group of the so-called Al-Li alloys, is featured with a very complex chemical composition. Hence, great differentiation in kinds and composition of inter-metallic strengthening phases which have a fundamental effect on the properties thereof, both for elastic and elastic-plastic ranges.

The microstructures of fracture surfaces reflect the complexity of the cracking mechanism at the initial stage of crack growth and propagation (in the notch-affected area), due to the interspersing of sections of ductile, brittle, and quasi-cleavage cracking, which here and there differ from typical images of fatigue fractures.

References

- ANDREWS E.W., GIBSON L.J. 2001. *The influence of cracks, notches and holes on the tensile strength of cellular solids*. Acta Materialia, 49: 2975-2979.
- DACKO M., BORKOWSKI W., DOBROCIŃSKI S., NIEZGODA T., WIECZOREK M. 1994. *Metoda elementów skończonych w mechanice konstrukcji*. Arkady, Warszawa.
- HERTZBERG R.W. 1983. *Deformation and Fracture Mechanics of Engineering Materials*. Second edition. John Wiley & Sons. New York/Chichester/Brisbane/Toronto/Singapore.
- KOCAŃDA S., KOCAŃDA A. 1989. *Niskocyklowa wytrzymałość zmęczeniowa metali*. PWN, Warszawa.
- Notch Effects in Fatigue and Fracture*. 2000. NATO Science Series II: Mathematics, Physics and Chemistry, Vol. 11. Kluwer Academic Publishers. Dordrecht/Boston/London.

- Peterson R. 1974. Stress concentration factors. Wiley, New York.
- PILKEY W. 1997. *Peterson's stress concentration factors*. Second edition. John Wiley & Sons. New York.
- SPENCER K., CORBIN S.F., LLOYD D.J. 2002. *Notch fracture behaviour of 5754 automotive aluminium alloys*. Materials Science & Engineering, A 332: 81-90,
- STRANDBERG M. 2002. *Fracture at V-notches with contained plasticity*. Engineering Fracture Mechanics, 69: 403-415,
- TLILAN H.M., YOUSUKE S., TAMOTSU M. 2005. *Effect of notch depth on strain-concentration factor of notched cylindrical bars under static tension*. European Journal of Mechanics A/Solids, 24: 406-416,
- TOKAJI K. 2005. *Notch fatigue behaviour in a Sb-modified permanent-mold cast A356-T6 aluminium alloy*. Materials Science & Engineering, A 396: 333-340,
- TROYANI N., HERNANDEZ S.I., VILLARROEL G., POLONAI Y., GOMES C. 2004. *Theoretical stress concentration factors for short flat bars with opposite U-shaped notches subjected to in-plane bending*. International Journal of Fatigue, 26: 1303-1310,
- ZIENKIEWICZ O.C. 1972. *Metoda elementów skończonych*. Arkady, Warszawa.

This study was performed within the framework of original working project No. 827/WAT/03.

Translated by Aleksandra Poprawska

Accepted for print 2006.04.20

